SLAC-PUB-5048
October 1989
(T/E)

B PHYSICS AT THE Z^0 POLE*

W. B. **ATWOOD**
Stanford Linear Accelerator Center,
Stanford University, Stanford, California 94309, USA
and
BENOIT MOURS
Stanford Linear Accelerator Center,
Stanford University, Stanford, California 94309, USA
and
Lab. de Phys. des Particules,
Annecy-le- Vieux, CEDEX, France

INTRODUCTION

The SLC has been running at SLAC since April, and more than 100 Z^0 events have been reconstructed. Shortly the new European facility at CERN-LEP-will also turn on, and by the end of the year we anticipate that more than 10,000 Z^0 events will have been registered by each of the four LEP detectors. Most of the experimental facilities at these two machines are equipped with excellent particle tracking and identification. Some have close-in tracking devices which will provide unparalleled precision in trajectory reconstruction, and lead to the possibility of identifying a large-proportion of the charmed and beauty particles.

Not only does the Z^0 pole offer a relatively large production cross section for e^+e^- machines, but a large proportion of the events (approximately 22% of the hadronic events) are $b\bar{b}$ pairs. In Fig. 1, the relative cross section for $e^+e^- \rightarrow Z^0 \rightarrow b\bar{b}$ is shown in comparison to the Υ_{4s} and Υ_{5s}. One sees from this figure that a gain of six or more is obtained from running at the Z^0. An SLC producing 10^5 events per year yields 20,000 $b\bar{b}$ events. Similarly, for LEP (running an order of magnitude higher in luminosity), over 200,000 $b\bar{b}$ events will become available per year. In addition,

Invited talk presented at the Workshop on B Physics,
Blois, France, June 26–July 1, 1989.

⋆ Work supported by Department of Energy contract DE–AC03–76SF00515.

the planned upgrade for LEP will increase its luminosity by about an order of magnitude, and the SLC will run with polarized electron beams.

The physics that may be studies from these event samples fall into two general categories: (1) tests of the Standard Model; and (2) studies of B mesons and B baryons, including lifetimes, mixing, spectroscopy, and CP violation.

STANDARD MODEL PHYSICS

Testing the Standard Model in the quark sector boils down to measuring the vector couplings of the quarks. Our present experimental knowledge of these couplings is poor and comes mostly from PEP/PETRA data.' The B events from Z^0 decay probably offer us the best laboratory in which to do Standard Model tests because it is relatively easy to separate B events from the other hadrons.

The rate for $Z^0 \rightarrow b\bar{b}$ is proportional to $(v_b^2 + a_b^2)$ where v_b (a_b) are the vector (axial) couplings of b quarks. With the Z^0 mass around 91 GeV,the electroweak mixing angle is increased and^2 $\sin^2 \theta_w \approx 0.235$. This yields

$$v_b^2 + a_b^2 = 1.47 \ ,$$

and

$$\frac{\Gamma(Z^0 \rightarrow bb)}{\Gamma(Z^0 \rightarrow \text{hadrons})} = 0.22 \ .$$

Specifically, if we measure the partial rate for $Z^0 \rightarrow b\bar{b}$ compared to $Z^0 \rightarrow \mu^+\mu^-$, we will have a good measurement of v_b.

From the above estimated rates, in 10^5 $Z^0 \rightarrow$ hadrons, 22,000 B events will be produced, together with 5000 $\mu^+\mu^-$ events. All the detectors at both SLC and LEP will be able to separate B events from the others by lepton tagging, and the efficiency for this can be estimated:

$$\epsilon_{tag} = N_b \times B_r(b \to lvx) \times \epsilon_{det}$$

$$= 2 \text{ x } 0.24 \text{ x } 0.50 \quad = \quad 0.24 \quad ,$$

where N_b is the number of b's per $Z^0 \to b\bar{b}$ event, $B_r(b \to lvx)$ is the semileptonic branching ratio for b's, and ϵ_{det} is the efficiency for the detector to clearly identify the lepton (most of the inefficiency in ϵ_{det} is due to the necessary minimum momentum cuts in P_t relative to the jet axis and P_{TOT}). The results will be a tagged b-event sample of about 5300.

Defining R to be

$$\mathbf{R} = \frac{\Gamma(Z^0 \to b\bar{b} \to lvx)}{\Gamma(Z^0 \to \mu^+\mu^-)} \simeq 1 \quad ,$$

the statistical error in R is just

$$\Delta R = R\left(\frac{1}{N_{b\bar{b}\to lvx}} + \frac{1}{N_{\mu^+\mu^-}}\right)^{1/2}$$

$$= 0.02R \quad = 0.02 \quad .$$

Thus

$$v_b^2 = 0.46 \pm 0.03 \quad ,$$

or

$$\frac{\Delta v_b}{v_b} \simeq 0.07 \quad .$$

The present error on v_b is $\sim \pm 1$.

Another technique can be used to measure v_b if polarized beams are available. The forward-backward charge asymmetry $A_{FB}^{b\bar{b}}$ integrated over 47r solid angle is proportional to v_b and is given by:

$$A_{FB}^{b\bar{b}} = \frac{3}{4} \cdot \frac{2v_e a_e}{v_e^2 + a_e^2} \cdot \frac{2v_b a_b}{v_b^2 + a_b^2} \quad ,$$

$$\simeq \frac{3}{4} \cdot (0.12) \cdot (-0.93) \quad = 0.084 \quad ,$$

where we used $\sin^2 \theta_w = 0.235$. This unpolarized asymmetry is quite small, but when the e^- beam can be polarized, the term with the electron couplings becomes

$$\frac{2v_e a_e}{v_e^2 + a_e^2} \left(= A_{LR}^{e^+e^-} \right) \rightarrow \frac{P_e + A_{LR}^{e^+e^-}}{1 + P_e A_{LR}^{e^+e^-}} \quad .$$

For an electron beam polarization P_e of 45%, the (0.12) given above for $A_{LR}^{e^+e^-}$ becomes 0.54 and

$$A_{FB}^{b\bar{b}} \ (45\%) \ = \ -0.38.$$

For-the case of a typical Z^0 detector, the angular coverage only extends to $|\cos\theta| < 0.9$, and $A_{FB}^{b\bar{b}}$ is slightly reduced:

$$A_{FB}^{b\bar{b}} \ (45\%)_{|\cos\theta| < 0.9} = -0.36 \quad .$$

To experimentally observe $A_{FB}^{b\bar{b}}$, care must be taken to include effects due to B^0 -mixing or to restrict the event sample to B_u mesons. For the present discussion, we choose the latter.

We have studied the experimental problems with a simulation of the SLD detector running at the SLC, but similar analysis for LEP detectors can be done. One of SLD/SLC's strongest advantages is the small beam-spot size. Another is how close to the interaction point the detectors may be placed[3] (SLD's inner layer of CCD detectors is at a radius of $\sim$ 27 mm). We find that inclusive B_u vertex reconstruction has an efficiency of $\gtrsim 30\%$ with an accuracy best described by a "separation" asymmetry:

$$A_{SEP} = \frac{N_{\text{corr}} - N_{\text{wrong}}}{N_{\text{corr}} + N_{\text{wrong}}} = 0.70 \quad ,$$

where $N_{\text{corr (wrong)}}$ are the number of b and $\bar{b}$ quarks correctly (wrongly) tagged. The separation asymmetry A_{SEP} delutes physics asymmetries ($A_{\text{OBS}} = A_{\text{SEP}} \cdot A_{\text{PHYS}}$) and the number of events necessary to make a physics asymmetry measurement to a given accuracy level is proportional to $1/A_{\text{SEP}}^2$.

Again using 10^5 Z^0 decays, about 4600 B_u vertices may be reconstructed, yielding $\Delta A_{FB}^{b\bar{b}}(45\%) \simeq 0.021$. Hence,

$$\left.\frac{\Delta v_b}{v_b}\right|_{45\%\ e^-\ \text{pol}} \simeq 0.05 \quad .$$

Even though these measurements of v_b are much better than that previously achieved, they will not constrain the Standard Model very much. In Fig. 2,

$$A_{LR}^{b\bar{b}} = \frac{2v_b a_b}{v_b^2 + a_b^2}$$

is plotted for various mass Z^0's as a function of the top quark mass (the Higg's mass was set at 100 GeV). The "data" point at m_t = 100 GeV with f0.05 error bar illustrates that about one order of magnitude reduction in the error will be necessary to probe the Standard Model in the quark sector.

B MESON PHYSICS POSSIBILITIES

As a prelude to this topic, we make a short digression to discuss topological reconstruction of *B* decays; details of the algorithms are given in another contribution to this conference (Ref. 4). *B* mesons will usually decay into a charmed particle, which then decays to the tracks, which we measure in our detectors. This two-stage decay process will result in "cascade topologies" as shown in Fig. 3.

The new tracking technologies — such as high resolution drift chambers, Silicon Strip Detectors, and CCD Vertex Detectors — promise to improve the precision of particles trajectories near the interaction point by up to an order of magnitude, and in some cases provide this precision in all three dimensions. We have only investigated this later case when "3D" information is present (as in the case of SLD). We believe it to be a critical element for solving the general vertex topology pattern recognition problem.

The-SLD will have four overlapping layers of CCD pixel devices for its vertex detector.[3] The pixel dimensions are about 22 μm on a side, and track coordinate resolutions as good as 6 μm seem to be possible. Every track with $|\cos\theta| < 0.85$ detected by the SLD Detector will have at least two pixel points on it. The problem of linking the pixel points to the main drift chamber tracks seems to be easily solved by requiring at least two pixels to lie on the extrapolated drift-chamber trajectory.

The present plans are to have a beam pipe of 25 mm radius, with the innermost layer of CCD's at $\approx$ 27 mm from the beam line. Earlier schemes to move in closer (us-.-. ing a 16-mm-radius beam pipe) have been tempered by the background measurement now available from the Mark II. It is easy to show that the resolution arising from finite measurement precision is proportional to r_o/l, where r_o in the radius of the inner most detector and l is the lever arm of the vertex detector. Also, the multiple scat- - tering error (which usually dominates) is proportional to r_o. The "rule-of-thumb" is simple: the vertexing precision is proportional to r_o. Thus, SLC has an intrinsic advantage over LEP, since vertex detectors can be a factor of two closer to the beam line.

Using a parametric simulation of the SLD detector to account for resolution effects and solid-angle coverage, LUND 6.3 Monte Carlo events of $Z^0 \rightarrow$ hadrons have been studied. The results reported here assume a beam pipe of 25 mm radius. A general topological pattern recognition program[4] was used to find cascade topologies in the simulated DST output banks. By comparing what was reconstructed with

the starting Monte Carlo input, various signal-to-noise and efficiency numbers were computed.

When a cascade topology is found, the chance that it is other than a $Z^0 \rightarrow b\bar{b}$ event is less than 5%. Hence, the contamination of u-, d-, s-, and c-quark final states is small (c-quarks dominate this background category). Since we consider this small contamination unimportant for the present, we ran the main sample of Monte Carlo events only for $Z^0 \rightarrow bb$. We processed 132,000 events; this would correspond to 600,000 $Z^0 \rightarrow$ hadrons interactions.

The more difficult problem is to identify correctly-found cascade topologies from incorrect combinations. To achieve a suitable signal-to-noise ratio, cuts were placed on the mass of the secondary vertex ($M_b > 2.8$ GeV), its total momentum ($P_{TOT} >$ 15 GeV/c), and the mass of the tertiary vertex (0.8 GeV $< M_c <$ 2.1 GeV). These cuts result in a sample of cascade topologies coming mainly from B mesons decaying into charm. Particle identification is used to identify and discard any topologies with net nonzero baryon number (net proton charge $\neq$ 0), and thus many B baryons are eliminated. Our final sample is composed of 92% B mesons and 7% B baryons.

In Table 1, we show where the topologies come from by referring back to the input Monte Carlo event. The table divides cascade topologies into nine categories corresponding to the nine possible charge combinations observed in the cascade. For each category, the Monte Carlo composition is shown divide as to particle/antiparticle and B meson type (u, d, or s). Already, one sees a significant enhancement of particle-versus-antiparticle and meson-type differentiation, simply on the basis of the charges of the reconstructed topologies.

B_u PHYSICS

By selecting cascade topologies which have $Q_b = \pm 1$, a sample of B_u mesons is obtained. The first and "simplest" measurement to make is the lifetime. The

experiment measures the flight path ($\gamma\beta c\tau$): the separation between the secondary vertex and the primary vertex. To estimate the boost factor ($\gamma\beta$), we have used the ratio of the observed momentum to the observed mass of the secondary vertex ($P_{TOT}(obs)/M_{obs}$)

There is uncertainty in this estimate, particularly in its resolution, coming from uncertainty in the fragmentation function of b-quarks into B-mesons. Overall, we estimate its contribution to the error on CT to be 50-60 μm. If more fully reconstructed B's are used, this error will shrink.

Our estimate of SLD's resolution in $c\tau$ for two different beam pipe diameters is shown in Fig. 4. The original plans called for a 16 mm radius pipe, but a more conservative design for the first runs with a 25 mm radius pipe is now being considered and has been used for this analysis. Offhand, one might expect the CT resolution to have simply scaled with the radius, but due to the uncertainly in the $\gamma\beta$ factor the loss in $c\tau$ resolution is less than 25/16. The signal-to-noise is degraded from 4.7/1 to 2.6/1 in the B_u sample for the larger beam pipe design.

The proper time ($c\tau$) for the B_u sample is shown in Fig. 5. Fitting this raw spectrum for $c\tau$ > 600 μm gives a lifetime of 355 $\pm$ 9 μm, to be compared to the 390 μm Monte Carlo input. The sample of B_u used for this exercise contained one B^0 for every 2.6 B_u's and, since their lifetimes were set to lower values (210 μm for B_d and 270 μm for- B_s), the measured value is pulled down by this contamination. We have not had time to develop methods for correcting this effect and, therefore, we will use the Monte Carlo lifetime values in this analysis. We also note that our mixing parameters will be different from the "book values" because of our use of nonstandard lifetimes.

B MESON MIXING AND A_{FB}

We begin this analysis by studying a case which has no mixing — the B_u mesons.

The distribution of events plotted against $Q_b \cos\theta$ is shown in Fig. 6(a). The large expected A_{FB} is obvious. The signal-to-noise ratio for this selection is about 2.1:1 in a sample of $\sim$ 5600 B_u candidates (a 7% reconstruction efficiency). The raw A_{FB} = 0.274 $\pm$ 0.014 which, upon correction for the background by a factor of [1 + (Signal/Noise)$^{-1}$], becomes

$$A_{FB}(\text{corr}) = 0.404 \pm 0.021 \ .$$

This is to be compared with the input to the Monte Carlo of 0.38. We should point out that our analysis doesn't include correction for:

- acceptance in the very forward/backward region;
- small asymmetries for the noise, which will slightly change our [1 + (Signal/Noise)$^{-1}$] correction factor

But these effects should be on the order of a few percent.

In Fig. 6(b), the data from Fig. 6(a) has been binned in units of $c\tau$ for the secondary, b vertex. No apparent dependence on, lifetime is present.

Separating neutral B-mesons into B_d's and B_s's is harder, and information from the particle identification systems plays a crucial role. It is found that the kaon content of the tertiary vertex allows for some separation. In the Monte Carlo, b-quarks fragment into B_d's 2.3 times more often than into B_s's. By requiring exactly one charged kaon to be associated with the tertiary vertex, D_s meson decays are suppressed, and a signal-to-noise ratio of 1.9 : 1 is achieved for the B_d sample. The 1928 reconstructed B_d's represent a reconstruction efficiency of about 3.6%.

The B_d events are plotted against $Q_c \cos\theta$ in Fig. 7(a), and a smaller, yet clearly visible, A_{FB} is seen. The raw A_{FB} for the B_d sample is 0.067 $\pm$ 0.019. Correcting for the finite signal to noise results in A_{FB} = 0.10 $\pm$ 0.03. This reduction in A_{FB} for B_d mesons compared to B_u mesons can be interpreted as due to B_d meson mixing and is described by $A_{FB}(\text{obs}) = A_{FB}(\text{phys})\ (1 - 2\chi)$. The extent to which

$$\frac{A_{FB}(\text{obs})}{A_{FB}(\text{phys})} < 1$$

is an indication that $\chi > 0$. If we take the A_{FB} measured with the B_u sample as the $A_{FB}(\text{phys})$, we find $\chi = 0.38 \pm 0.04$. Since the mixing phenomenon requires time to develop, the cut made in the vertex finding of flight paths greater than 0.5 mm introduces a distortion in the measurement of χ. Simply put, by requiring a minimum flight path for the B-mesons, the direct B^0 decays are preferentially discarded with respect to the mixed case of $B^0 \rightarrow \bar{B}^0 \rightarrow$ decay. A correction for this finite lifetime requirement on vertex finding can be estimated from the Monte Carlo, and for B_d mesons is found to be 0.26. Applying the correction gives $\chi_{\text{meas}} = 0.10 \pm 0.01$, to be compared with the Monte Carlo input of 0.09.

Proceeding now as for the B_u *case,* $A_{FB}(B_d)$ is binned in units of CT and is shown in Fig. 7(b). We see the $B_d \rightarrow \bar{B}_d$ oscillation directly for the first time. A fit to this data of the form

$$A_{FB} = A_{B_d} \cos(\Delta m_{B_d} t)$$

gives a $\chi^2/\text{df} = 4.4/7$ df. The significance of the fit $(A_{B_d}/\sigma A_{B_d})$ is 7.0 and the oscillation parameter is $\Delta m_{B_d}/\Gamma_{B_d} = 0.44 \pm 0.04$. The expected number for $\Delta m_{B_d}/\Gamma_{B_d}$ is 0.48. The merit of this technique over the time integrated method is that systematic errors will be small: errors in the measurement of $c\tau$ are cancelled to first order in the ratio of Am/I' and errors in the amplitude of the effect have little bearing on the oscillation rate.

A sample of B_s mesons is extracted from the neutral B mesons by requiring the association of a pair of oppositely charged K mesons with the tertiary (charm) vertex. About half of these K pairs came from ϕ mesons and the rest are randomly distributed at higher masses. No cut is made on the K-pair mass. A sample of 204 B_s candidates results, with a signal-to-noise ratio

of 1.3:1. In Fig. 8(a),the events are shown versus $Q_c \cos\theta$, similar to that plotted for the B_d sample. The apparent A_{FB} is 0.05 $\pm$ 0.07, which (after background correction) becomes 0.09 $\pm$ 0.12. The mixing probability deduced from this A_{FB} is χ_{B_s} = 0.39 $\pm$ 0.15. Again the finite vertex flight path introduces a correction, which is now smaller, due to the more rapid B_s oscillation rate, and is estimated to be 0.92 from the Monte Carlo. Hence, $\chi_{B_s}(\mathrm{corr})$ = 0.36 $\pm$ 0.14, to be compared to 0.46, the input to the Monte Carlo.

Figure S(b) shows $A_{FB}(B_s)$ plotted versus cr. We observe the rapid B_s oscillation. A fit of the form

$$A_{FB} = A_{B_s} \cos(\Delta m_{B_s} t)$$

gives a χ^2/df = 1.5/5 df. The fit significance $(A_{B_s}/\sigma A_{B_s})$ is 3.6. The oscillation parameter is $\Delta m_{B_s}/\Gamma_{B_s}$ = 3.37 $\pm$ 0.14, to be compared to 3.4, the Monte Carlo input. The error is relatively smaller here than in the B_d case, because the B_s data ranges over $\sim$ 2 periods where, in the B_d case, only half a period was fit. Again, the systematic errors are thought to be small.

CP VIOLATION EFFECTS IN *B* MESONS

CP violation is an indication of an asymmetry between the particle world and the antiparticle world. In the case of neutral B-meson decay rates, asymmetries such as

$$A_{CP} = \frac{\Gamma(B^0 \to f) - \Gamma(\bar{B}^0 \to \bar{f})}{\Gamma(B^0 \to f) + \Gamma(\bar{B}^0 \to \bar{f})}$$

are the experimental manifestations of this difference. In the three-generation Standard Model, similar combinations of parameters occur either to suppress a branching mode believed to exhibit large CP violation or to make the CP violation very small.

The number of events $N_{b\bar{b}}$ required to observe N_σ standard deviations can be expressed as

$$N_{b\bar{b}} = A_{CP}^{-2} N_\sigma^2 A_{sep}^{-2} \cdot \frac{1}{2B_r(B^0 \to f)} \frac{1}{\epsilon_f} \frac{1}{\epsilon_{tag}} \frac{1}{\sigma_{B^0}} ,$$

where σ_{B^0} is the probability of a b-quark fragmenting to a B^0, ϵ_f is the final state reconstruction efficiency, ϵ_{tag} is the particle-antiparticle tagging efficiency, and $Br(B^0 \to f)$ is the branching fraction to the final state f. Estimates for $N_{b\bar{b}}$ range from 10^7–10^9, due to either the smallness of $Br(B^0 \to f)$ or of A_Q.

Presently, only LEP, run for high luminosity at the Z^0, has the possibility of producing event samples that begin to reach these numbers.

CONCLUSIONS

The decay $Z^0 \to b\bar{b}$ offers perhaps the best example in the quark sector to study the Standard Model coupling. Unfortunately, the statistical uncertainty from data samples thought to be available next year will only allow tests of the general coupling scheme, and will be too large to provide a precision test. The feasibility of measuring particle-antiparticle mixing for both neutral B-mesons has been demonstrated. Together with the mixing measurements, excellent determinations of B_u, B_d and B_s lifetimes can easily be made. The event samples necessary to pursue these studies are well within the design luminosity reach of both the SLC and LEP.

On the other hand, studies of CP violation in B-meson decay is thought to require event samples which will barely be achieved by a LEP upgraded to high luminosity.

ACKNOWLEDGMENTS

The authors express thanks to P. Grosse-Wiesmann and I. Dunietz for many stimulating and helpful discussions. G. Bower deserves thanks for installing B^0 mixing in the LUND Monte Carlo. Thanks also are due to the SLC Polarization Group and to the SLD Collaboration.

REFERENCES

1. BLOCKUS, D. et al. 1986. Proposal for polarization at SLC. SLAC Report SLAC-PROP-l.

2. We used M_t = 100 GeV and M_{Higgs} = 100 GeV.

3. SLD Design Report SLAC-273. 1984 and updates.

4. **ATWOOD,** W. B. 1989. *B* identification by topology with the SLC detector. These proceedings; SLAC-PUB-5047.

5. **ALBRECHT,** H. et al. ARGUS Collaboration. 1987. Phys. Lett. 192B: 245. See also **KATAYAMA,** N. CLEO Collaboration. $B^0\bar{B}^0$ mixing and charmless *B* meson decay into baryons from CLEO. 1988 SLAC Summer Institute.

6. SJÖSTRAND, T., & **BENGTSSON,** M. (Lund Univ.). 1987. Comput. Phys. Commun. 43: 367.

7. The effect of *B* mixing on A_{FB} has been analyzed by BIGI, I. I. Y., & **CVETIC,** M. 1986. Phys. Rev. D34: 1651.

8. **ATWOOD,** W. B., **DUNIETZ,** I. & GROSSE–WIESMANN, P. 1988. SLAC–PUB-4544.

Table I. Breakdown of cascade topology events by secondary and tertiary vertex changes, Q_b and Q_c. For each charge combination, the sample is resolved into particles and antiparticles, as well as the meson flavors B_u, B_d, and B_s (see upper left entries under Q_b = Q_c = -1 for key).

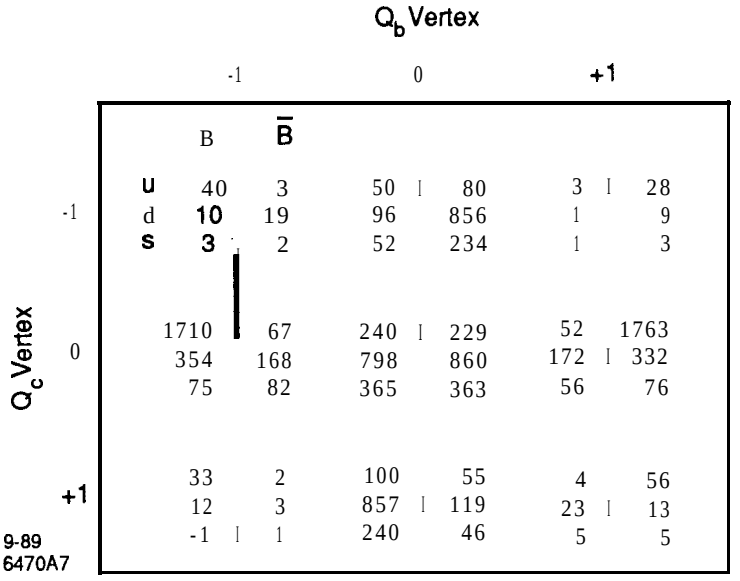

FIGURE CAPTIONS

Fig. 1. Production cross sections for $e^+e^- \rightarrow Z^0 \rightarrow b\bar{b}$ with 45% left-handed polarized electrons and $e^+e^- \rightarrow b\bar{b}$ with unpolarized beams at Υ_{4s} and Υ_{5s}. Cross sections are plotted with relative offsets to these resonances.

Fig. 2. $A_{LR}^{b\bar{b}}$ as a function of the top quark mass for various Z^0 masses: from 89 GeV (for the lowest curve) to 93 GeV (top curve), by steps of 1 GeV.

Fig. 3. A cascade B-meson decay topology: (a) the primary vertex, (b) the secondary B-meson decay vertex (neutral prongs are shown as dashed lines), and (c) the tertiary charmed meson decay vertex.

Fig. 4. B-meson lifetime resolution in proper time $(c\tau)$ for (a) a 16-mm-radius beam pipe, and (b) a 25-mm-radius beam pipe.

Fig. 5. Measured $c\tau$ for the B_u sample. The line is the result of the fit for events with $c\tau > 600$ μm.

Fig. 6. A_{FB} for the B_u meson sample: (a) the time-integrated sample plotted against $Q_b \cos\theta$ and (b) the data from (a) analyzed for A_{FB} and plotted versus $c\tau$ derived from the B_u meson vertex. The solid line indicates the time-integrated average for the sample.

Fig. 7. A_{FB} for the B_d meson sample: (a) the time integrated sample plotted against $Q_c \cos\theta$ and (b) the data from (a) analyzed for A_{FB} and plotted versus $c\tau$ derived from the B_d meson vertex. The solid line is a fit to this data (see text).

Fig. 8. A_{FB} for the B_s meson sample: (a) the time-integrated sample plotted against $Q_c \cos\theta'$ and (b) the data from (a) analyzed for A_{FB} and plotted versus $c\tau$ derived from the B_s meson vertex. The solid line is a fit to this data (see text).

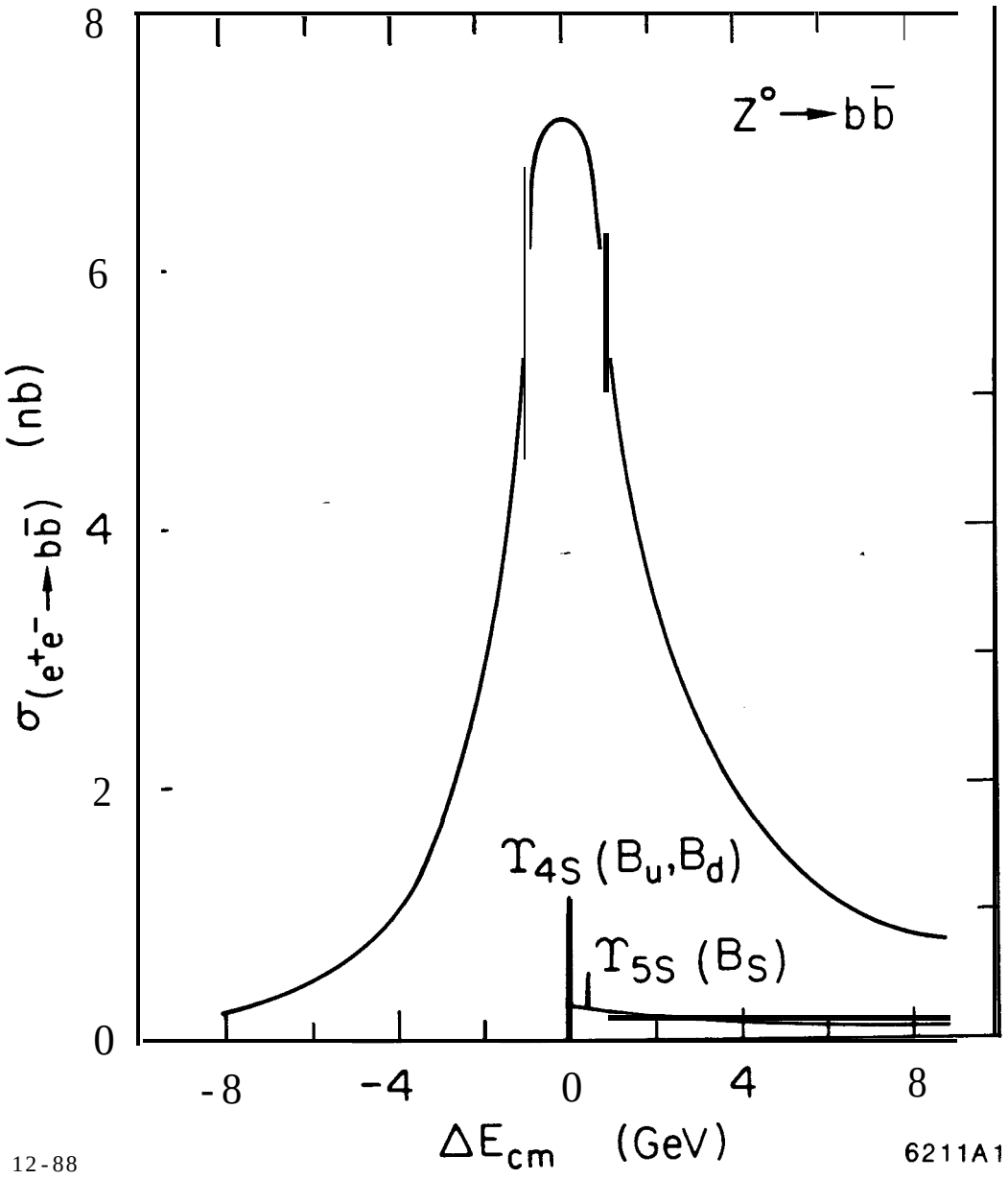
8
6
4
2
0
$\sigma_{(e^+e^- \to b\bar{b})}$ (nb)
$Z^\circ \to b\bar{b}$
Υ_{4S} (B_u, B_d)
Υ_{5S} (B_S)
-8
-4
0
4
8
ΔE_{cm} (GeV)
12-88
6211A1

Fig. 1

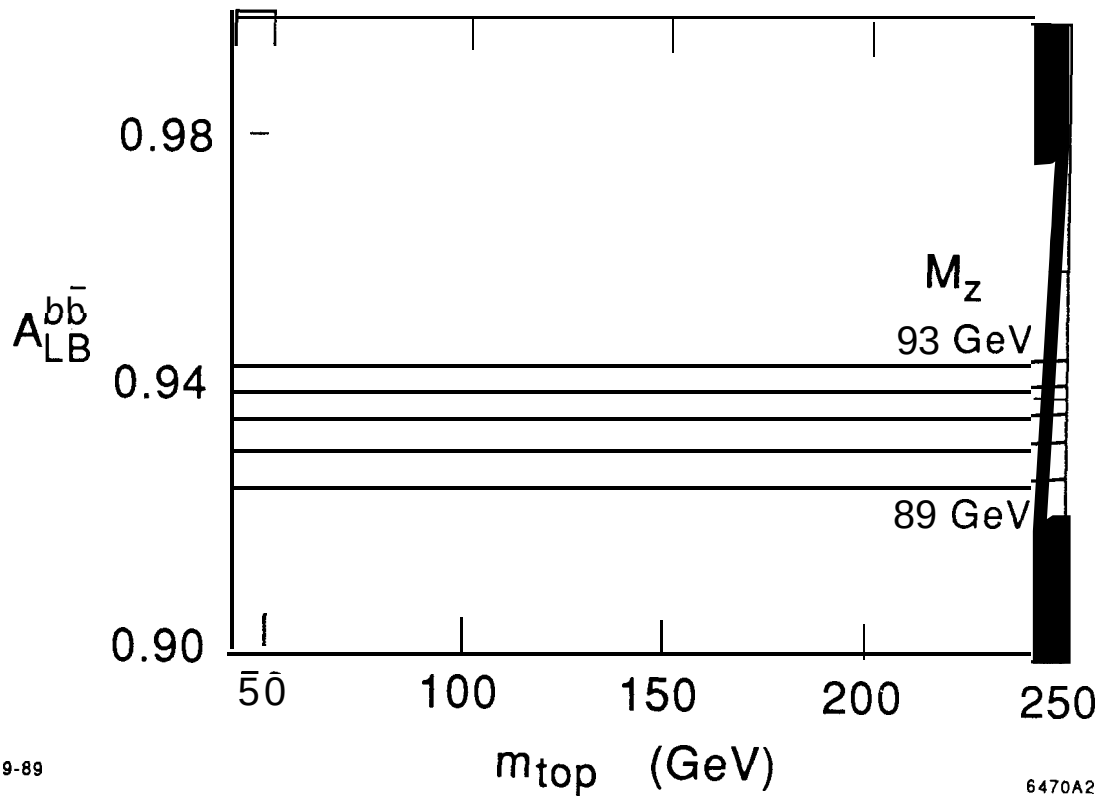
0.98
0.94
0.90
$A_{LB}^{b\bar{b}}$
M_z
93 GeV
89 GeV
50
100
150
200
250
m_{top} (GeV)
9-89
6470A2

Fig. 2

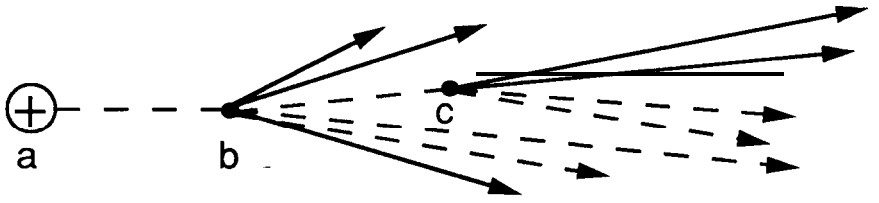

10-88 6141A1

Fig. 3

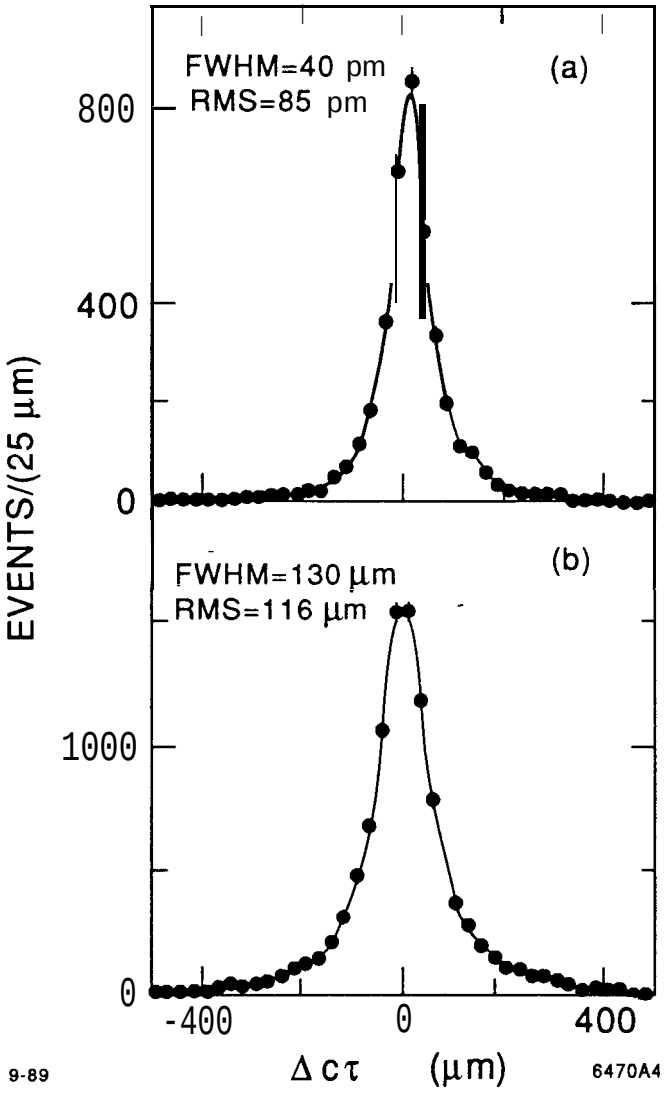
FWHM=40 pm
RMS=85 pm
(a)
800
400
0
EVENTS/(25 μm)
FWHM=130 μm
RMS=116 μm
(b)
1000
0
-400
0
400
Δcτ (μm)
9-89
6470A4

Fig. 4

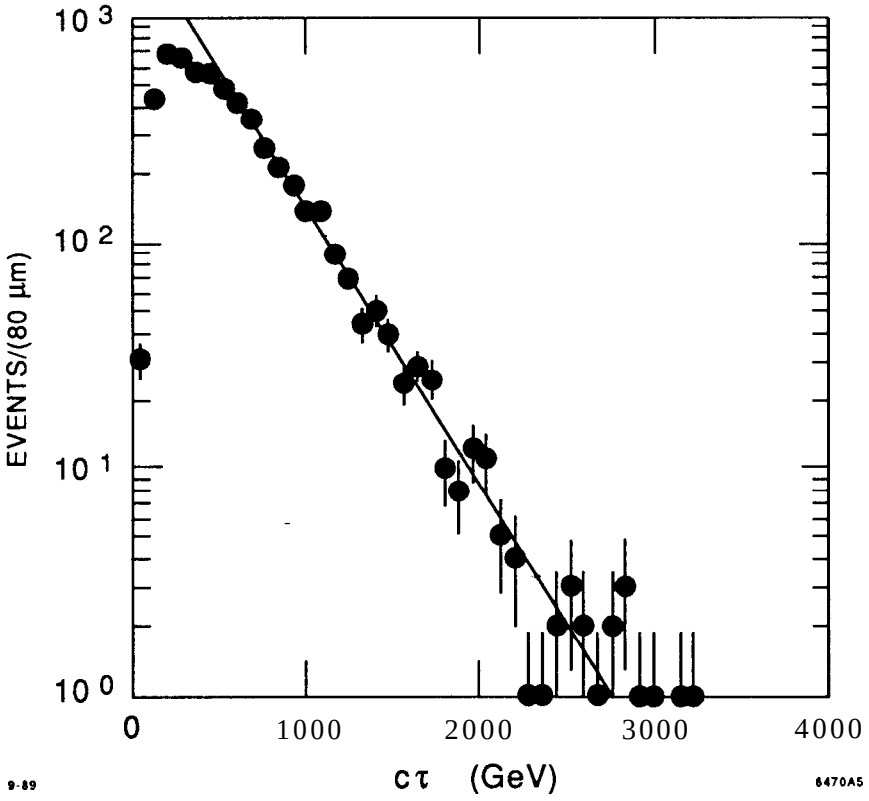
10 3
10 2
10 1
10 0
EVENTS/(80 μm)
0
1000
2000
3000
4000
cτ (GeV)
9-89
6470A5

Fig. 5

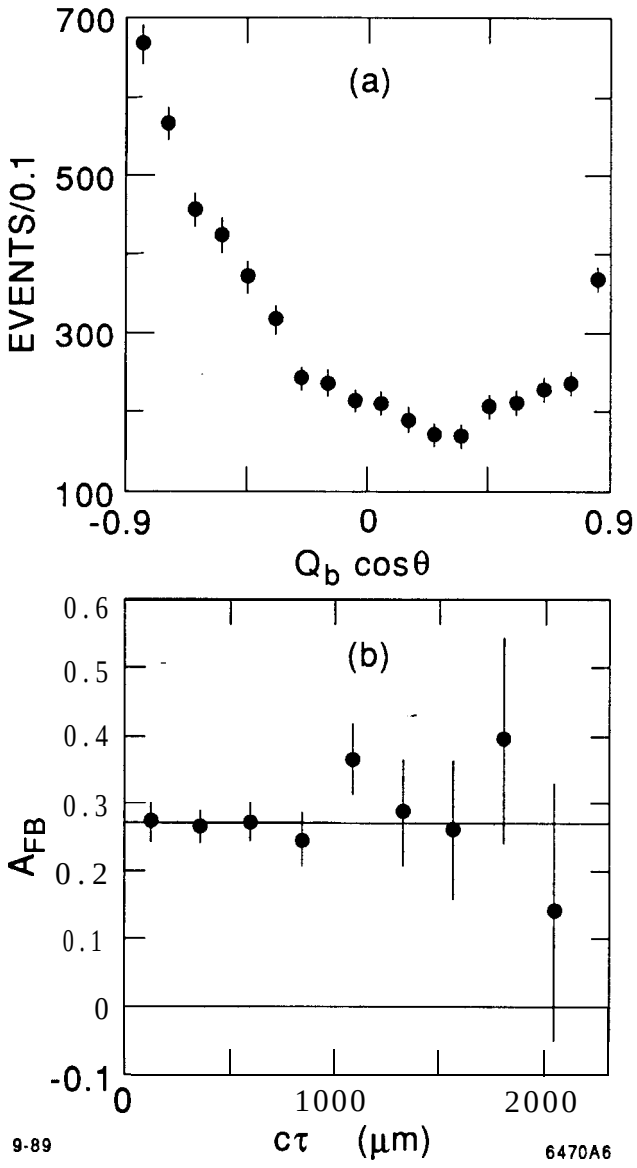
700
500
300
100
EVENTS/0.1
(a)
-0.9
0
0.9
$Q_b \cos\theta$
0.6
0.5
0.4
0.3
0.2
0.1
0
-0.1
A_{FB}
(b)
0
1000
2000
$c\tau$ (μm)
9-89
6470A6

Fig. 6

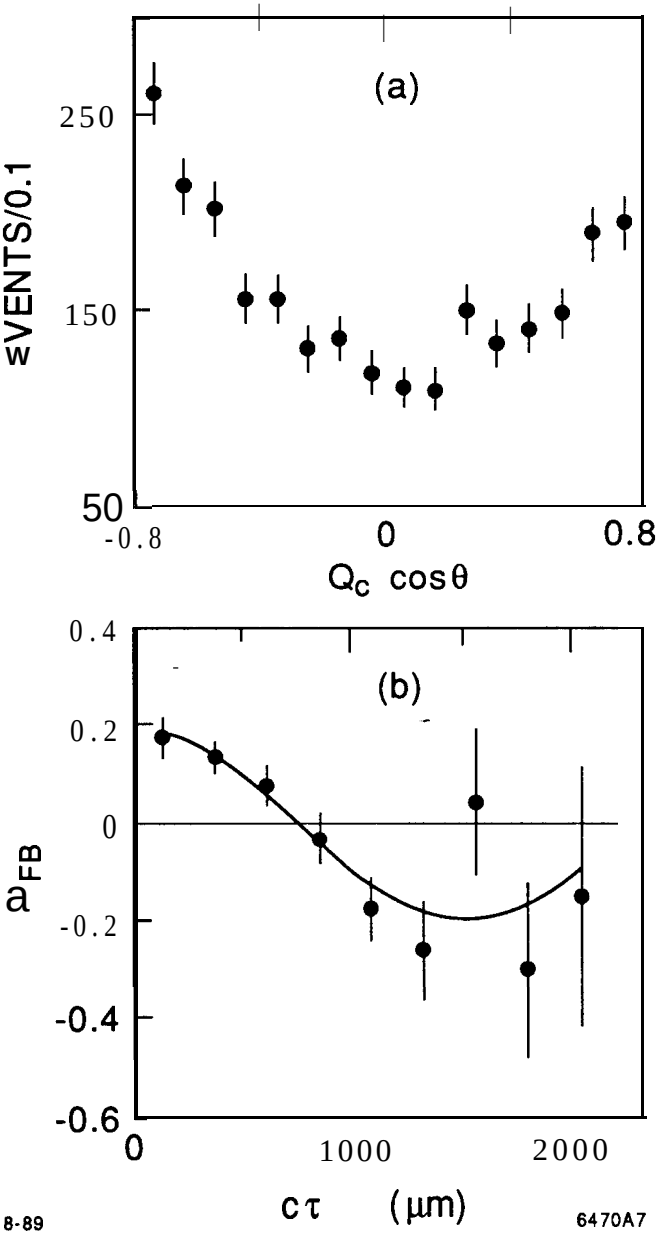
(a)
250
150
50
EVENTS/0.1
-0.8
0
0.8
$Q_c \cos\theta$
(b)
0.4
0.2
0
-0.2
-0.4
-0.6
a_{FB}
0
1000
2000
$c\tau$ (μm)
8-89
6470A7

Fig. 7

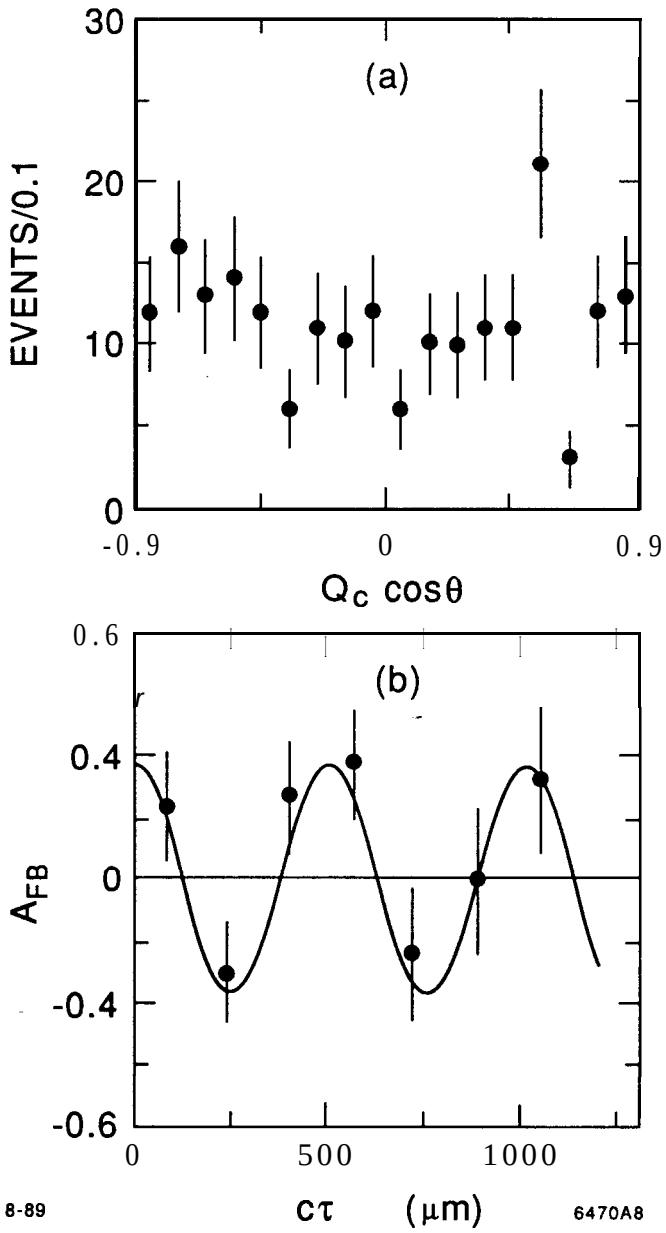
30
20
10
0
EVENTS/0.1
(a)
-0.9
0
0.9
$Q_c \cos\theta$
0.6
0.4
0
-0.4
-0.6
A_{FB}
(b)
0
500
1000
cτ (μm)
8-89
6470A8

Fig. 8